Progress In Electromagnetics Research B, Vol. 47, 339–357, 2013

DESIGN AND TIME-DOMAIN ANALYSIS OF COMPACT MULTI-BAND-NOTCHED UWB ANTENNAS WITH EBG STRUCTURES

Lin Peng* **and Chengli Ruan**

Institute of Applied Physics, University of Electronic Science and Technology of China (UESTC), Chengdu 610054, China

Abstract—Four ultra-wideband (UWB) antennas are proposed: one referenced antenna without notch and three novel antennas with one, two and three notched bands, respectively. The UWB referenced antenna consists of a beveled rectangular metal patch, a 50 Ω microstrip line and a defective ground plane. Then, by utilizing one, two and three electromagnetic band-gap (EBG) structures on the UWB antenna, the antennas present one, two and three notched-band responses, respectively. The frequency domain characteristics including VSWR, transfer coefficient S_{21}, radiation patterns and group delay are investigated. It is found that the EBG design approach is a good candidate for frequency rejection at the certain frequencies, owing to high performance of notch design and the notched-band bandwidth control abilities. Meanwhile, these abilities also enable less useful frequencies rejected. The design examples exhibit good band-rejected characteristics in the WiMAX/WLAN interference bands (3.4, 5.2 and 5.8-GHz bands). Moreover, good time-domain characteristics of the antennas are checked based on group delay, waveform response, correlation coefficient and pulse width stretch ratio (SR).

1. INTRODUCTION

Ultra-wideband (UWB) communication systems have became a most promising candidate for short-range high-speed indoor data communications since the US-FCC released the bandwidth 3.1–10.6 GHz in 2002. Therefore, as a key component of UWB communication systems, UWB antennas have attracted a great many interest [1–4]. However, the existence of other wireless narrowband

Received 30 November 2012, Accepted 5 January 2013, Scheduled 10 January 2013
* Corresponding author: Lin Peng (penglin528@hotmail.com).

standards that already occupy frequencies in the UWB band, such as wireless local-area network (WLAN, 5.2-GHz (5150–5350 MHz) and 5.8-GHz (5725–5825 MHz) bands) and worldwide interoperability for microwave access (WiMAX, 3.3–3.6 GHz), requires rejection of certain frequencies within the UWB band. The conventional techniques for band-notched design include: cutting slots on the patch/ground plane [5–10], putting parasitic elements close to the radiator [11–14] and embedding filter in the feeding line [15]. These techniques are efficient for notched-band design. However, it is hard to conquer the two main problems generalized in [14] for frequency rejected function design: 1) the obstacles in achieving efficient dual/multi band-notched design (due to strong couplings between band-notched structures) and 2) notched-band bandwidth control for single-, especially dual-notch design.

To overcome the two problems of frequency rejected function design, our previous paper introduced a new kind of UWB band-notched antenna design by placing electromagnetic band-gap (EBG) structures couple to the microstrip feeding line [16]. The presented approach is very efficient for single/dual band-notched design as it exhibits advantages in notched-band tuning, as well as notched-band bandwidth control by adjusting the coupling gap or the distance between the EBG and the upper edge of the ground plane. It is found that the given approach in [16] have superiority in solving the two problems, compared to other designs.

However, the sizes of the antennas in [16] are large, and discrepancies between simulated and measured VSWRs were observed due to the tolerance of the substrate parameters. Importantly, time-domain characteristics, critical to determine the qualification of the antenna for practical UWB applications, were not investigated for the proposed approach. Moreover, the convenient approach in [16] is unfortunately not able be applied in triple notched-band design. Therefore, new solutions are necessary and there are much works need to be done. The purposes of this study are: 1) to reconfirm the validity of the proposed design approach by using RO4003C substrate (relative permittivity $\varepsilon_r = 3.38$ and loss tangent $\tan\delta = 0.0027$), 2) to design band-notched antennas that are more compact in size and more suitable for practical applications, 3) to use new solution to rejected the WiMAX band that was not rejected in [16], 4) for time-domain analysis of the antennas and demonstration of the proposed design approach suitable for pulse transmission and 5) to provide several band-notched UWB antennas options for applications in the environments with different interference bands.

A novel UWB antenna more compact than that in [16] is designed

in this study by a beveled rectangular metal patch and defective ground plane. The corner-located vias mushroom-type EBG (CLV-EBG) structure is utilized for frequency-rejected function design as it is more compact than the edge-located vias mushroom-type EBG (ELV-EBG) structure by moving via from edge to corner [16, 17]. Then, by placing one or two CLV-EBG structures coupling to the microstrip feeding line of the UWB antenna, single or dual notches are obtained as desired. However, the design of [16] reaches its restriction when triple notches are required as a third EBG structure has severe coupling with its neighbor, which will severely depress the design efficiency. Therefore, the third notched-band was achieved by new solution of placing the third EBG structure on the radiating patch as learning from [18]. Then, a triple band-notched UWB antenna is successfully design. The band-notched antennas were constructed and measured. The experimental results show reasonable agreements with simulated ones and the validity of the proposed design approach for band-notched UWB antenna design. At last, time-domain characteristics of the antennas are investigated by analyzing and comparing their group delay, transfer coefficient S_{21}, waveform response, correlation coefficient and pulse width stretch ratio (SR). The antennas demonstrate good time-domain performances. Therefore, high efficiency of the given design approach for UWB band-notched antenna design is proved.

2. ANTENNA DESIGN AND RESULTS

2.1. UWB Antenna Design and Results

The configuration of the UWB antenna (denoted as antenna 1) is shown in Figure 1(a). The antenna was constructed on an $h = 0.8\,\text{mm}$ Rogers RO4003C substrate with a relative permittivity $\varepsilon_r = 3.38$ and a loss tangent $\tan\delta = 0.0027$. As shown in the figure, L_0 and W_0 denote the total length and width of the antenna, respectively. A beveled rectangular radiator is fed by a $50\,\Omega$ microstrip line. On the other side of the substrate, a rectangular ground plane only covers the section of the microstrip feeding line. A defection with dimension $L_d \times W_d$ is etched on the ground plane for impedance matching improvement over a broad frequency range. The width of the gap between the radiator and the ground plane is g. The antenna can be easily fabricated by Printed Circuit Board (PCB) technique with very low cost.

The parameters of antenna 1 are: $W_0 = 22\,\text{mm}$, $L_0 = 32\,\text{mm}$, $h = 0.8\,\text{mm}$, $L_1 = 11.5\,\text{mm}$, $L_2 = 8.5\,\text{mm}$, $W_1 = 5\,\text{mm}$, $W_f = W_d = 1.8\,\text{mm}$, $L_d = 3.5\,\text{mm}$, and $g = 0.5\,\text{mm}$. The simulated results of the antennas with and without defection are illustrated in Figure 1(b).

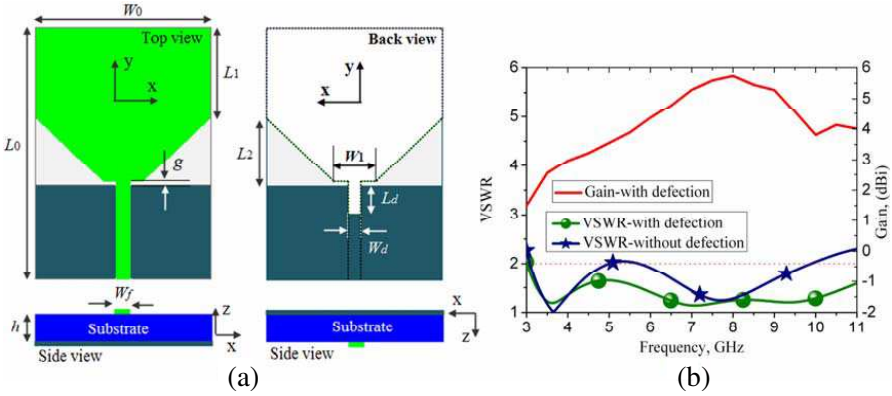

Figure 1. Antenna. (a) Configuration and (b) simulated results with and without defection.

It is found that both antennas with and without defection obtain good impedance matching in a very wide bandwidth. However, the one with defection (antenna 1) demonstrates a better VSWR curve. The operating band of antenna 1 covers the entire UWB band (3.1–10.6 GHz) and goes beyond the required 10.6 GHz with VSWR < 2. The peak gain of antenna 1 is also exhibited in Figure 1(b), ranging from 2 dBi to 5.7 dBi in the entire UWB band.

2.2. Single Band-notched UWB Antenna Design and Results

If the applied environment only exist one narrow WLAN interference band (200 MHz for 5.2-GHz band and 100 MHz for 5.8-GHz band), it is better to utilize UWB antennas with single narrow notched-band to ensure little useful frequencies wasted and consequently acquire better antenna performance with interference still relieved. Unfortunately, most of the in existing single band-notched UWB antennas fail to afford a narrow notched-band with useful frequencies also rejected. Therefore, these antennas are not the best choice. To overcome these drawbacks, two UWB antennas with single narrow notched-band are designed based on the given approach.

The configuration of the proposed single notched-band UWB antenna (denoted as antenna 2) is demonstrated in Figure 2(a). As shown in the figure, a CLV-EBG cell is placed close to the microstrip feeding line with a gap e_{g1}. The patch dimensions of the CLV-EBG are a_1 and b_1. The distance between upper edge of the ground plane and the EBG patch is d_{g1}. A via with radii r is located at the lower-right corner of the EBG patch. Note that when the EBG structure

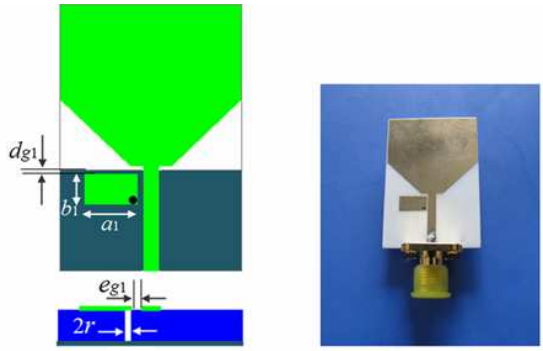

(a) (b)

Figure 2. Antenna 2. (a) Configuration and (b) photograph of Case 2.

is applied to the antenna, there is no repeated work required for the previous determined dimensions. As will be demonstrated in the current distributions of Section 2.5, the current of the notch-frequency is concentrated on the EBG, which causes the antenna to be non-responsive at that frequency, then, a notched-band is obtained as desired.

Two cases of antenna 2 with single narrow notched-band correspond to 5.2 and 5.8-GHz WLAN interference bands, respectively, are designed with parameters as follow:

Case 1 (5.2-GHz band): $a_1 = 7.1$ mm, $b_1 = 3.5$ mm, $e_{g1} = 0.3$ mm, $r = 0.3$ mm and $d_{g1} = 0$ mm.

Case 2 (5.8-GHz band): $a_1 = 6.3$ mm, $b_1 = 3.5$ mm, $e_{g1} = 0.3$ mm, $r = 0.3$ mm and $d_{g1} = 0$ mm.

It is found that Case 1 and Case 2 have the same configuration and dimensions except EBG patch length a_1. The simulated VSWRs of Case 1 and Case 2 are exhibited in Figure 3(a). As shown in the figure, desired filtering functions are introduced without influence to the UWB properties. The notch frequencies of Case 1 and Case 2 are happened at 5.31 GHz (4.97–5.37 GHz, VSWR > 2) and 5.86 GHz (5.54–5.93 GHz, VSWR > 2), respectively. Therefore, the 5.2-GHz and 5.8 GHz WLAN bands are successfully rejected, respectively. Moreover, the notch-frequency can be conveniently adjusted by the EBG patch, and the width of the notched-band can also be tuned by adjusting the parameters e_{g1} and d_{g1} [16]. Sharp reductions of the peak gain curves in their corresponding notched-bands are observed as well as good performances at the other frequencies, as expected.

Case 2 of antenna 2 is fabricated as shown in Figure 2(b) to verify the simulations. A SMA connector is soldered at the end of

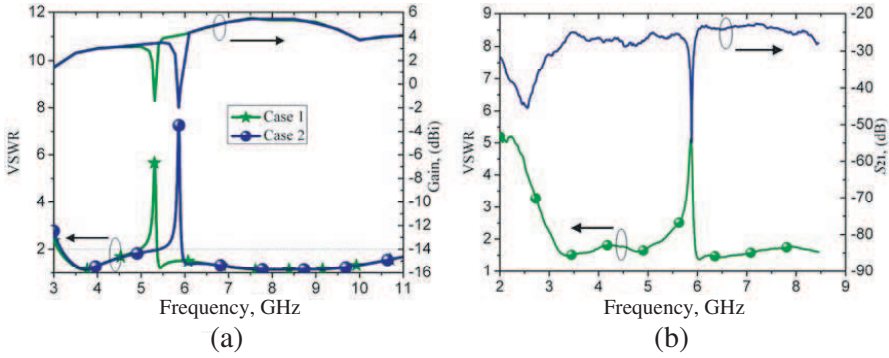

Figure 3. Results of antenna 2. (a) Simulated results of Case 1 and Case 2 and (b) measured results of Case 2.

the microstrip feeding line for measurement. It must be pointed out that, the measurements in this paper were conducted by an Agilent E5071C ENA series network analyzer with the highest measurable frequency at 8.5 GHz. Though it does not cover the whole UWB band (3.1–10.6 GHz), it reaches our requirements as the concerned notched-band locate in the measurable band. The measured VSWR curve is exhibited in Figure 3(b). A notch-frequency is observed at 5.86 GHz (5.50–5.94 GHz, VSWR $>$ 2), while good impedance matching is obtained at other frequencies. Therefore, it is in good agreement with the simulated result. The transfer coefficient S_{21} of the antenna is also measured and illustrated in Figure 3(b), which presents a sharp decrease of more than 30 dB at the notch as well as flat responses at the other frequencies. Note that the transfer coefficient is obtained by orientating two identical antennas face-to-face with a distance of 95 mm.

2.3. Dual Band-notched UWB Antenna Design and Results

When there exist two WLAN bands intervene UWB systems, band-notched UWB antennas with single wide notched-band or dual narrow notched bands can be used to mitigate the interferences. For single band-notched UWB antenna, a wide notched-band with its notch-frequency located between the lower and upper WLAN bands to cover the two interference bands, which result in useful frequencies between the lower and upper WLAN bands also rejected. Besides, its interference alleviation function is discounted as the notch-frequency not happened in the interference bands. Dual band-notched UWB antennas do not have these problems as its two notch-frequencies

happened in the two WLAN bands, respectively, as well as useful frequencies between the two WLAN bands radiate with no constraint. Therefore, UWB antenna with dual narrow notched bands is a better choice.

The proposed dual band-notched UWB antenna designed to reject both the 5.2 and 5.8-GHz bands is exhibited in Figure 4, and referred as antenna 3. Compared to antenna 2, another CLV-EBG structure with dimension of $a_2 \times b_2$ is utilized for additional notch generation. The optimized design parameters are: $a_1 = 6.3\,\text{mm}$, $b_1 = 3.5\,\text{mm}$, $a_2 = 7.1\,\text{mm}$, $b_2 = 3.5\,\text{mm}$, $e_{g1} = 0.3\,\text{mm}$, $e_{g2} = 0.4\,\text{mm}$, $d_{g1} = d_{g2} = 0\,\text{mm}$ and $r = 0.3\,\text{mm}$. Noted that, since the mutual coupling between the two EBG structures are very small, the notches design parameters of antenna 3 that correspond to Case 1 and Case 2 of antenna 2 are identical, except small modification on e_{g1}.

The simulated VSWR curve of antenna 3 is demonstrated in Figure 5(a). Two notch frequencies are observed at 5.31 GHz (4.98–5.35 GHz, VSWR $>$ 2) and 5.86 GHz (5.69–5.92 GHz, VSWR $>$ 2), with WLAN bands rejected and useful frequencies between them pass through. It is found that the antenna's low and high notch frequencies are identical to Case 1 and Case 2 of antenna 2, respectively, which indicate coupling between the two CLV-EBGs is small. Peak gain curve of antenna 3 demonstrates sharp decrease in the notched-bands, and coincide with antenna 1 at other frequencies.

The measured results of the fabricated antenna 3 in Figure 4(b) are illustrated in Figure 5(b). It is found from the VSWR curve that two notch-frequencies at 5.23-GHz (4.97–5.28 GHz, VSWR $>$ 2) and 5.86-GHz (5.66–5.92 GHz, VSWR $>$ 2) are obtained, though variation

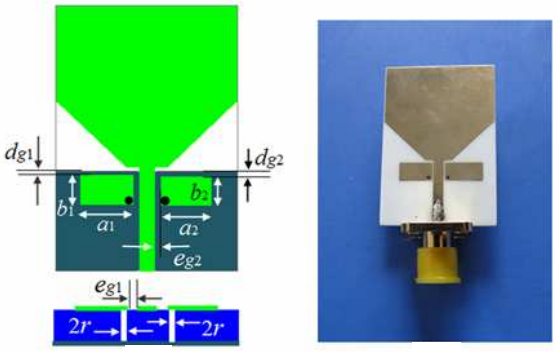

Figure 4. Antenna 3. (a) Configuration and (b) photograph.

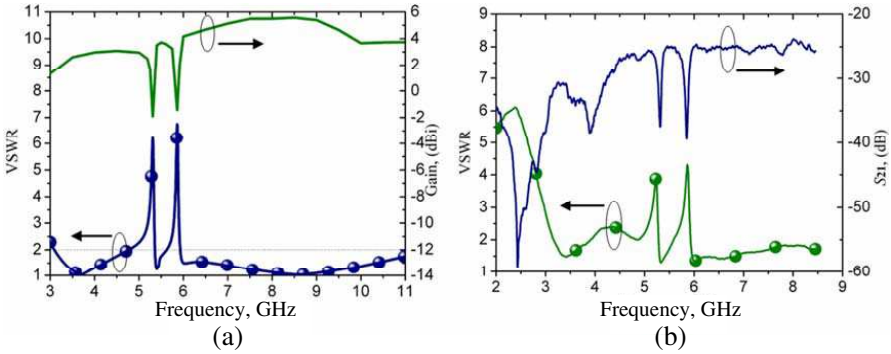

Figure 5. Results of antenna 3. (a) Simulated results and (b) measured results.

of VSWR curve around 4.3 GHz with VSWR values up to 2.36 are observed. The transfer coefficient S_{21} is also shown in Figure 5(b). Two sharp decreases with nearly 15 dB attenuation are obtained at the corresponding measured notch-frequencies. However, sharp decrease of transfer coefficient is also observed around 3.9 GHz. The causes of these variations are most probably due to the solder roughness of the SMA connector and experimental tolerance. However, the measured results as well as those of antenna 2 had validated the correctness of the simulations and the validity of the design.

2.4. Triple Band-notched UWB Antenna Design and Results

Triple notched-bands are greatly desired for UWB antennas when the operational environment exist both WLAN and WiMAX interference bands. Though antenna 2 and 3 have demonstrated efficiency on single/dual notches design by utilizing one/two EBG structures couple to the microstrip line, it is hard to produce a third notch to antenna 3 by applying a third EBG cell coupling to the microstrip feeding line due to strong coupling between the third EBG cell and its neighbor makes it difficult to tune the notches. Therefore, the third EBG structure was placed on the radiating patch as shown in Figure 6 [18]. The third EBG patch is beveled rectangular shaped and coplanar with the ground plane. A via with radius of r is utilized to connect the EBG patch and the radiating patch. The labels of the beveled rectangular EBG patch are indicated in the figure while other labels can be referred to antenna 1 and 3 for simplicity. Then, an UWB antenna with triple notched bands was successful designed (denoted as antenna 4).

As small coupling occurs between the beveled rectangular EBG

and the other two CLV-EBGs, small modifications on the notch designs are necessary. Still, there is no repeated work required on the UWB antenna. The optimized design parameters are: $a_1 = 6.8\,\text{mm}$, $b_1 = 3.5\,\text{mm}$, $a_2 = 6.1\,\text{mm}$, $b_2 = 3.5\,\text{mm}$, $e_{g1} = 0.5\,\text{mm}$, $e_{g2} = 0.3\,\text{mm}$, $d_{g1} = d_{g2} = 0\,\text{mm}$, $r = 0.3\,\text{mm}$, $a_3 = 2\,\text{mm}$, $a_4 = 8\,\text{mm}$, $b_3 = 2\,\text{mm}$, $b_4 = 7.15\,\text{mm}$ and $d_{g3} = 0.3\,\text{mm}$.

The simulated VSWR curve of antenna 4 is illustrated in Figure 7(a). Three notched-bands are obtained to mitigate interferences from 3.4, 5.2 and 5.8-GHz bands. The three notch frequencies are 3.40 GHz (3.31–3.53 GHz, VSWR $>$ 2), 5.32 GHz (5.02–5.36 GHz, VSWR $>$ 2) and 5.81 GHz (5.66–5.90 GHz) without influence on antenna's UWB performances. The peak gain of antenna

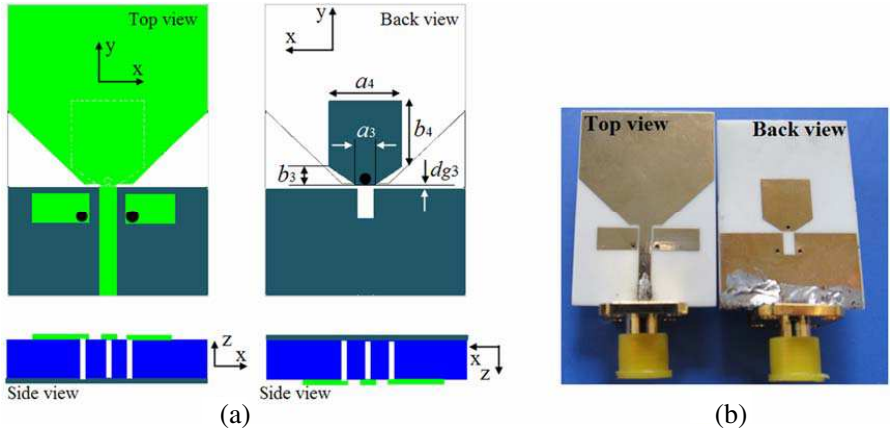

Figure 6. Antenna 4. (a) Configuration and (b) photograph.

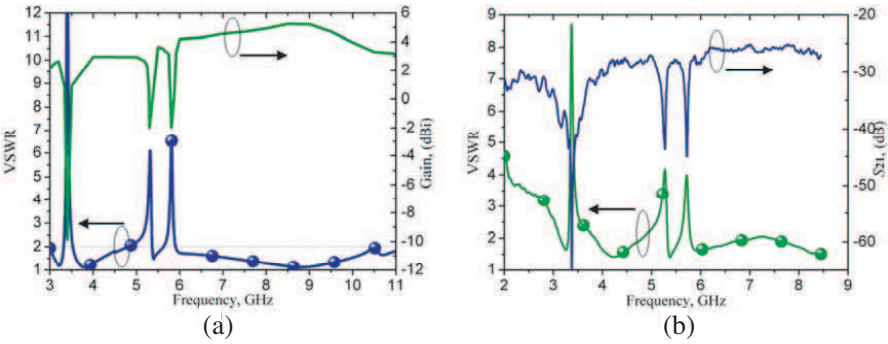

Figure 7. Results of antenna 4. (a) Simulated results and (b) measured results.

4 is also plotted in Figure 7(a) and sharp decreases occur at the three notched-bands as predicted.

The photograph of the fabricated antenna 4 is exhibited in Figure 6(b). The measured results are shown in Figure 7(b). It is found that it is in reasonable agreement with the simulated results with three notch frequencies at 3.37 GHz (3.30–3.69 GHz, VSWR > 2), 5.27 GHz (4.97–5.32 GHz, VSWR > 2) and 5.71 GHz (5.60–5.79 GHz, VSWR > 2). The transfer coefficient S_{21} of antenna 4 is measured with sharp decreases at the three notch frequencies as expected. The attenuation for the first WiMAX band is about 35 dB, while the attenuations for the two WLAN bands are approximately 15 dB.

2.5. Comparisons of Current Distribution and Radiation Patterns

To further investigate the band-notched operational mechanism and the effects of the EBG structures on antenna performances, current distributions of antenna 1 and antenna 4 were plotted in Figure 8

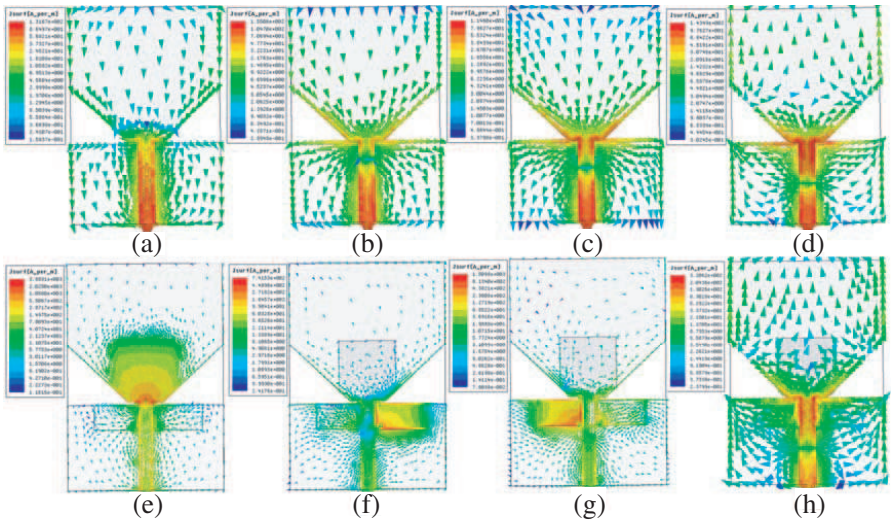

Figure 8. Comparison of current distributions between antenna 1 and antenna 4. (a)–(d) Demonstrate current distributions of antenna 1, while (e)–(h) demonstrate current distributions of antenna 4. (a) 3.4 GHz of antenna 1. (b) 5.32 GHz of antenna 1. (c) 5.81 GHz of antenna 1. (d) 7.5 GHz of antenna 1. (e) 3.4 GHz of antenna 4. (f) 5.32 GHz of antenna 4. (g) 5.81 GHz of antenna 4. (h) 7.5 GHz of antenna 4.

for comparison. Figures 8(a)–(d) present current distributions of antenna 1 at 3.4 GHz, 5.32 GHz, 5.81 GHz and 7.5 GHz, respectively, while Figures 8(e)–(h) demonstrate current distributions of antenna 4 at the corresponding frequencies, respectively. By carefully comparing the current distributions of antenna 1 and antenna 4, it is found

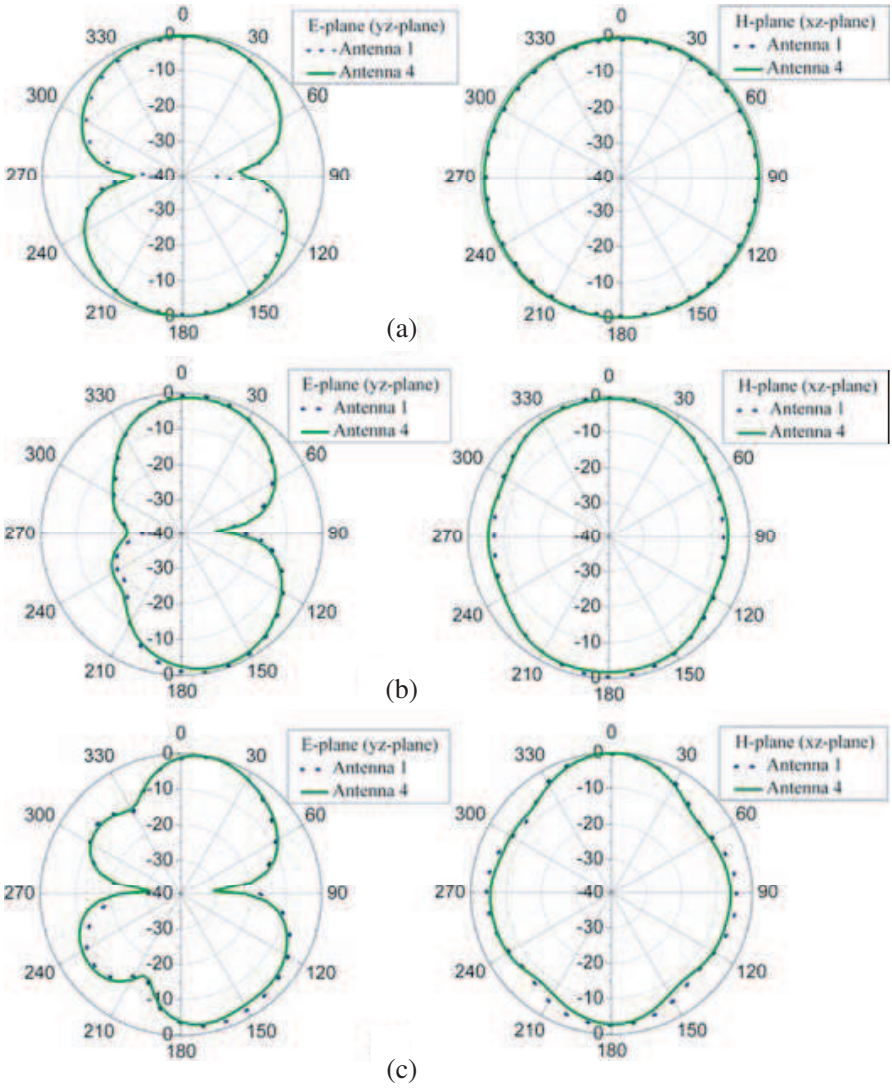

Figure 9. Comparison of radiation patterns between antenna 1 and antenna 4. (a) 3.2 GHz, (b) 7.5 GHz and (c) 10 GHz.

that they have similar current distribution at the pass-band frequency 7.5 GHz, and the current is weak at the notch deigns (EBGs) at the frequency. However, the current distributions of notch-frequencies 3.4 GHz, 5.32 GHz and 5.81 GHz are concentrated on their corresponding EBG structures with little distributed on other portions of the antennas. Therefore, we can conclude from Figure 8 that the introduction of EBG structures for notches design has little effects on the UWB antenna performances at the pass-band frequency, while arousing large reflection at the desired notch-frequencies as well as indicating easy notch frequency tuning by the EBG structure.

Pass-band radiation patterns of the UWB band-notched antennas are important indicators for evaluating the effects of the notch designs (EBGs) on the antenna's pass-band performances. Therefore, radiation patterns of antenna 1 and 4 at 3.2, 7.5, and 10 GHz are plotted in Figure 9 for comparison. The antennas are printed in the xy-plane, and they are y-polarized as the monopoles are in the y-direction. Therefore, the E-plane for these antennas is the yz-plane and the H-plane is the xz-plane. The used coordinate is indicated in Figure 1. It is found from the figure that the radiation patterns of antenna 4 are identical with their counterparts of antenna 1. Besides, the antennas exhibit omni-directional radiation patterns though some distortions are observed at 7.5 and 10 GHz. Thus, we can conclude from the figure that the introduction of EBG has little effect on the radiation patterns, then, the design is very efficient.

3. TIME-DOMAIN ANALYSIS

The investigation of frequency-domain characteristics such as reflection coefficient, radiation patterns and gain, are sufficient to evaluate antenna's performances for traditional applications. However, for UWB applications such as short-range high-speed indoor data communication systems and ground-penetrating radars, where a transient pulse signal (such as Gaussian pulse) is utilized for signal transmission and reception, waveform response of an UWB antenna are also very critical to determine the qualification of the antenna for practical applications [19–23]. Therefore, time-domain analysis of UWB antennas is with great significance especially for UWB band-notched antennas whose waveform can easily be distorted by antenna characteristics of rejection bands. In this section, group delay, waveform responses, correlation coefficient and pulse width stretch ratio (SR) are performed to evaluate time-domain characteristics of the proposed antennas. Notice that, the so-called antenna 2 in this section is the Case 2 of antenna 2 in Section 2.2.

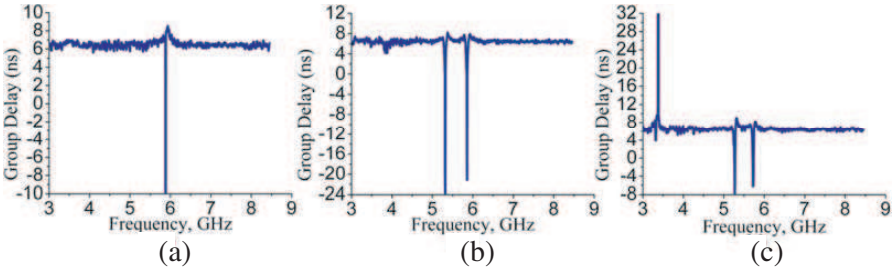

Figure 10. Measured group delay of the proposed antennas. (a) Antenna 2. (b) Antenna 3. (c) Antenna 4.

3.1. Group Delay

To avoid waveform distortion, a linear phase response (constant group delay) is desired. Therefore, group delay curves of antenna 2, 3 and 4 are measured to characterize their time-domain property. The results are exhibited in Figure 10. Sharp variations of group delay at the notch-frequencies are observed, which can break down the constant group delay requirement. However, the variation of the measured group delays is less than 1 ns in the pass-band, which indicates good linear phase responses. Moreover, widths of the sharp variation of group delay are narrow. Therefore, waveform distortion due to non-linear phase response is very small, even negligible. Besides, learnt from the frequency-domain responses (VSWR and transfer coefficient S_{21}), it is found that the notched-band bandwidths are narrow with more useful frequencies transmitted while compare to most of the reported designs, therefore, waveform distortion due to nulls of frequency spectrum is minimized.

3.2. Waveform Response

As UWB antennas are inspired by transient Gaussian pulse, waveform response provides intuitionistic recognition on antennas time-domain performance is favourable. Therefore, waveform responses of the antennas are demonstrated in this section for comparison. The input signal at the transmitting antenna terminal is illustrated in Figure 11. This Gaussian pulse signal has a frequency spectrum from 3.1–10.6 GHz. Then, the signals at the receiving antenna terminals are illustrated in Figure 12(a) for comparison. The waveforms are obtained by placing a pair of identical antennas face-to-face with a distance 0.6 m. It is found from the figure that, the ringing effects are happen to the band-notched antennas 2–4. However, ringing distortions are

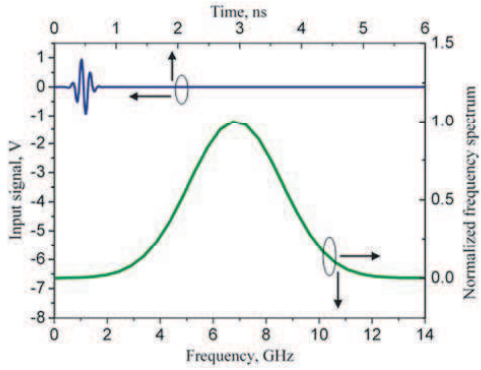

Figure 11. Input signal at the transmitting antenna terminal.

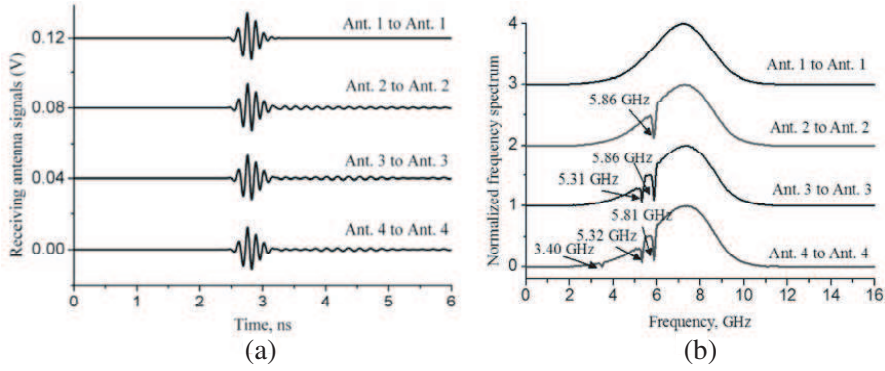

Figure 12. Comparison of the waveform responses and frequency spectra. (a) Waveform responses and (b) frequency spectra. Note that the waveforms and frequency spectra curves are shifted in Y-axis.

very small and the energy is concentrated in the vicinity of the peak. Therefore, the notch designs (EBGs) have little effects on waveform distortion and the antennas present good pulse-preserving capability. To appraise time-domain performances of the antennas more objectively, correlation coefficient and pulse width stretch ratio (SR) values are calculated in the following Section 3.3 and Section 3.4, respectively. The frequency spectra of the receiving signals are also plotted as shown in Figure 12(b). As shown in the figure, notches of frequency spectra are observed at corresponding notched-bands.

3.3. Correlation Coefficient

The correlation coefficient is more quantitative about waveform distortion of the antennas. It compare the waveforms of transmitting antenna input signal and the receiving signal (the electric field intensity signal or the receiving antenna signal) at far-field region [19–21].

Correlation coefficient of signals $s_1(t)$ and $s_2(t)$ is defined by

$$\rho = \max_{\tau} \left\{ \frac{\int s_1(t)s_2(t-\tau)dt}{\sqrt{\int s_1^2(t)dt}\sqrt{\int s_2^2(t)dt}} \right\} \tag{1}$$

where τ is a delay which is varied to make numerator in (1) a maximum [22].

As the antennas show omni-directional radiation patterns, then only the H-plane (xz-plane) correction coefficient is calculated and depicted for simplicity. Table 1 presents the results for various angles derived from input signal at the transmitting antenna terminal and the far-field receiving signal. The electric field intensity signals are obtained by placing virtual probes at the far-field (0.6 m) of the transmitting antenna, while the receiving antenna signal is acquired by orientating two identical antennas face-to-face with a distance of 0.6 m. For ideal condition, the correlation coefficient is up to 1. It is found from the table that the values of the correlation coefficient are larger than 0.88, and both the results derived from electric field intensity signal and receiving antenna signal are good. Besides, our another major point is to seek effect of the EBG structures on time-domain characteristics. Thus, by comparing the correlation coefficient of antenna 1 and those of the band-notched antennas, it is found that negative effects in antenna's pulse-preserving capability from the introduction of EBG structures are very small.

Table 1. The correlation coefficient values for the proposed antennas (xz-plane).

	Electric field intensity signal					Receiving antenna signal
	0°	45°	90°	135°	180°	Face-to-face
Antenna 1	0.9896	0.9705	0.9103	0.9611	0.9881	0.9541
Antenna 2	0.9731	0.9626	0.8898	0.9537	0.9758	0.9265
Antenna 3	0.9709	0.9609	0.9042	0.9543	0.9740	0.9195
Antenna 4	0.9719	0.9624	0.9056	0.9531	0.9753	0.9224

3.4. Pulse Width Stretch Ratio (SR)

In UWB communication systems, the temporal width of transmitted impulses is very important for high-speed data transmission [19]. Therefore, calculating pulse width stretch ratio (SR) is great significance to judge UWB antenna capability as well as to evaluate superiority of notch-design approaches.

The SR is defined by the ratio of pulse width of the far-field receiving signal to the width of the source voltage [19, 20]. For a signal $s(t)$, let the normalized cumulative energy function $E_s(t)$ be defined by:

$$E_s(t) = \frac{\int\limits_{-\infty}^{t} |s(t')|^2 dt'}{\int\limits_{-\infty}^{+\infty} |s(t')|^2 dt'} \tag{2}$$

Then, the SR for time window width of 90% energy captured between far-field receiving signal $s_2(t)$ to transmitting antenna signal $s_1(t)$ is given by:

$$\text{SR} = \frac{E_{s2}^{-1}(0.95) - E_{s2}^{-1}(0.05)}{E_{s1}^{-1}(0.95) - E_{s1}^{-1}(0.05)} \tag{3}$$

The SR values in H-plane (xz-plane) are calculated as shown in Table 2. It is found that SR values for electric field intensity signal vary from 1.03 to 1.25 at the detecting angles and SR values for receiving antenna signal varies from 1.45 to 1.62. These results are good and much better that those in [20, 21]. Besides, the introduction of EBG structure for notch design has small impacts on the antenna SR values.

Through time-domain analysis in this section, such as group delay, waveform response, correlation coefficient and values of

Table 2. The pulse width stretch ratio (SR) values for the proposed antennas (xz-plane).

	Electric field intensity signal					Receiving antenna signal
	0°	45°	90°	135°	180°	Face-to-face
Antenna 1	1.03	1.07	1.05	1.10	1.05	1.45
Antenna 2	1.06	1.11	1.25	1.16	1.09	1.62
Antenna 3	1.07	1.12	1.23	1.15	1.10	1.62
Antenna 4	1.06	1.10	1.22	1.16	1.10	1.58

SR, we had certified outstanding time-domain performance of the proposed antennas with good pulse-preserving capability while reject interferential frequencies. It is also found that the introduction of EBG structures have very small negative effects on time-domain characteristics. Therefore, the given design approach shows advantages.

4. CONCLUSION

Several compact band-notched UWB antennas with one, two and three notched bands were designed based on EBG structure for specific applications with different interference bands. A compact UWB antenna is also design as reference. The efficient dual/triple notches design ability and notched-band bandwidth control capacity of the given approach enable us to design single/dual/triple narrow notched-band UWB antennas reject the narrow interference bands and enable more useful frequencies radiated. The band-notched antennas are constructed and tested with acceptable agreement between the simulated and measured results. Moreover, the time-domain characteristics of the antennas are investigated with good performances. Besides, the studies reveal the proposed design approach have little effect time-domain characteristics and pass-band frequency-domain characteristics, which confirm the high efficiency of the proposed design. Therefore, the proposed antennas are good candidates for UWB pulse transmission with electromagnetic interferences from nearby WiMAX/WLAN communication systems mitigated.

ACKNOWLEDGMENT

This work was supported by the Fundamental Research Funds for the Central Universities under Grant E022050205 and CSC Project 2011607056.

REFERENCES

1. Vorobyov, A. V. and A. G. Yarovoy, "Human body impact on UWB antenna radiation," *Progress In Electromagnetics Research M*, Vol. 22, 259–269, 2012
2. Chen, Z. N., T. S. P. See, and X. M. Qing, "Small printed ultrawideband antenna with reduced ground plane effect," *IEEE Trans. Antennas Propag.*, Vol. 55, No. 2, 383–388, 2007.

3. Liang, J. X., C. C. Chiau, X. D. Chen, and C. G. Parini, "Study of a printed circular disc monopole antenna for UWB systems," *IEEE Trans. Antennas Propag.*, Vol. 53, No. 11, 3500–3504, 2005.
4. Abbosh, A. M. and M. E. Bialkowski, "Design of ultrawideband planar monopole antennas of circular and elliptical shape," *IEEE Trans. Antennas Propag.*, Vol. 56, No. 1, 17–23, 2008.
5. Ghatak, R., A. Karmakar, and D. R. Poddar, "A circular shaped Sierpinski carpet fractal UWB monopole antenna with band rejection capability," *Progress In Electromagnetics Research C*, Vol. 24, 221–234, 2011.
6. Yang, G., Q.-X. Chu, and T.-G. Huang, "A compact UWB antenna with sharp dual band-notched characteristics for lower and upper WLAN band," *Progress In Electromagnetics Research C*, Vol. 29, 135–148, 2012.
7. Chu, Q. X. and Y. Y. Yang, "A compact ultrawideband antenna with 3.4/5.5 GHz dual band-notched characteristics," *IEEE Trans. Antennas Propag.*, Vol. 56, No. 12, 3637–3644, 2008.
8. Peng, L., C. L. Ruan, and X. C. Yin, "Analysis of the small slot-loaded elliptical patch antenna with a band-notched for UWB applications," *Microw. Opt. Technol. Lett.*, Vol. 51, No. 4, 973–976, 2009.
9. Zhang, S.-M., F.-S. Zhang, W.-Z. Li, T. Quan, and H.-Y. Wu, "A compact UWB monopole antenna with WiMAX and WLAN band rejections," *Progress In Electromagnetics Research Letters*, Vol. 31, 159–168, 2012.
10. Tilanthe, P., P. C. Sharma, and T. K. Bandopadhyay, "A monopole microstrip antenna with enhanced dual band rejection for UWB applications," *Progress In Electromagnetics Research B*, Vol. 38, 315–331, 2012.
11. Yazdi, M. and N. Komjani, "A compact band-notched UWB planar monopole antenna with parasitic elements," *Progress In Electromagnetics Research Letters*, Vol. 24, 129–138, 2011.
12. Liu, W. X. and Y.-Z. Yin, "Dual band-notched antenna with the parasitic strip for UWB," *Progress In Electromagnetics Research Letters*, Vol. 25, 21–30, 2011.
13. Peng, L., C. L. Ruan, Y. L. Chen, and G. M. Zhang, "A novel band-notched elliptical ring monopole antenna with a coplanar parasitic elliptical patch for UWB applications," *Journal of Electromagnetic Waves and Applications*, Vol. 22, No. 4, 517–528, 2008.
14. Ryu, K. S. and A. A. Kishk, "UWB Antenna with single or dual

band-notches for lower WLAN band and upper WLAN band," *IEEE Trans. Antennas Propag.*, Vol. 57, No. 12, 3942–3950, 2009.

15. Qu, S. W., J. L. Li, and Q. Xue, "A band-notched ultrawideband printed monopole antenna," *IEEE Antennas Wireless Propag. Lett.*, Vol. 5, 495–498, 2006.
16. Peng, L. and C. L. Ruan, "UWB band-notched monopole antenna design using electromagnetic-bandgap structures," *IEEE Trans. Microw. Theory Tech.*, Vol. 59, No. 4, 1074–1081, 2011.
17. Rajo-Iglesias, E., L. Inclan-Sanchez, J. L. Vazquez-Roy, and E. Garcia-Muoz, "Size reduction of mushroom-type EBG surfaces by using edge-located vias," *IEEE Microwave Wireless Comp. Lett.*, Vol. 17, No. 9, 670–672, 2007.
18. Thomas, K. G. and M. A. Sreenivasan, "A simple ultrawideband planar rectangular printed antenna with band dispensation," *IEEE Trans. Antennas Propag.*, Vol. 58, No. 1, 27–34, 2010.
19. Kwon, D. H., "Effect of antenna gain and group delay variations on pulse-preserving capabilities of ultrawideband antennas," *IEEE Trans. Antennas Propag.*, Vol. 54, No. 8, 2208–2215, 2006.
20. Yang, Y. Y., Q. X. Chu, and Z. A. Zheng, "Time domain characteristics of band-notched ultrawideband antenna," *IEEE Trans. Antennas Propag.*, Vol. 57, No. 10, 3426–3430, 2009.
21. Zheng, Z. A., Q. X. Chu, and Z. H. Tu, "Compact band-rejected ultrawideband slot antennas inserting with $\lambda/2$ and $\lambda/4$ resonators," *IEEE Trans. Antennas Propag.*, Vol. 59, No. 2, 390–397, 2011.
22. Telzhensky, N. and Y. Leviatan, "Novel method of UWB antenna optimization for specified input signal forms by means of genetic algorithm," *IEEE Trans. Antennas Propag.*, Vol. 54, No. 80, 2216–2225, 2006.
23. Kumar, M., A. Basu, and S. K. Koul, "UWB printed slot antenna with improved performance in time and frequency domains," *Progress In Electromagnetics Research C*, Vol. 18, 197–210, 2011.